# Supplementary material for: Modelling decadal trends and the impact of extreme events on carbon fluxes in a deciduous temperate forest using the QUINCY model

Tea Thum[1], Tuuli Miinalainen[1], Outi Seppälä[1], Holly Croft[2], Sheryl Rogers[3], Ralf Staebler[4], Silvia Caldararu[5], and Sönke Zaehle[6]

[1]Finnish Meteorological Institute, Helsinki, Finland
[2]University of Sheffield, Sheffield, The United Kingdom
[3]McMillan University, Canada
[4]Environment and Climate Change Canada
[5]Trinity College, Dublin, Ireland
[6]Max Planck Institute for Biogeochemistry, Jena, Germany

## S1 Implementation of age in the development of leaf chlorophyll

To slow down the development of the leaf chlorophyll in spring, we used leaf age factor, $L_f$, that was defined as a function of mean leaf age $L_{age}$ (in days):

$$L_f = MIN(0.2 + 0.8 * L_{age}/d_{10}, 1.0) \tag{S1}$$

where $d_{10}$ is a parameter defining for how long time the $L_f$ will be less than one. By matching the development of the simulated leaf chlorophyll to the observed leaf chlorophyll, it was estimated to be 10 days. This $L_f$ was then further used to adjust the fractions for the nitrogen usage as follows. The fraction for the structural part was adjusted to be

$$fN_{struc,cl} = k_0^{struc} + (1.0 - k_0^{struc})(1.0 - L_f) - k_1^{struc} L_f N_{leaf,cl} \tag{S2}$$

with the other parameter and variable names remaining as in Eq. 3. The fraction allocated to chlorophyll ($fN_{chl}$) was adjusted to:

$$fN_{chl} = \frac{k_0^{chl} - k_1^{chl} e^{-k_{fn}^{chl} LAI_{cl}}}{a_{chl}^n L_f} \tag{S3}$$

with the other parameter and variable names remaining as in Eq. 4.

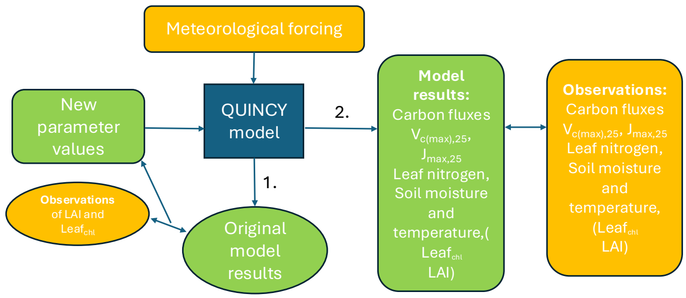


**Figure S1.** A schematic figure showing the workflow of the study. The model box is in dark blue, observation related variables in orange and model related variables in light green ovals. First (arrow denoted with 1) the original model results are compared to the observed LAI and $Chl_{Leaf}$ and after that the model is run again with some new parameter values. After this (arrow denoted with 2) the model results are compared to different observations.

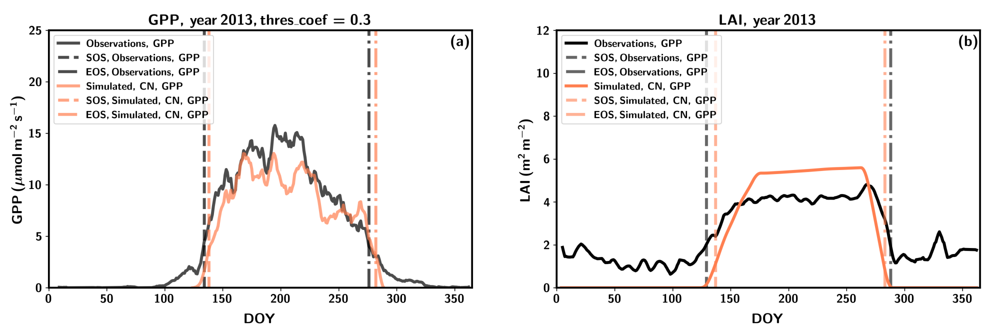


**Figure S2.** Seasonal cycle of GPP (a) and LAI (b) in 2013, smoothed with a seven-day averaging window. Black lines are observations and orange lines are QUINCY model results. The start of season (SOS) days are denoted by black (observations) and orange (simulations) vertical dashed lines. The end of season (EOS) days are denoted by black (observations) and orange (simulations) dash-dotted lines.

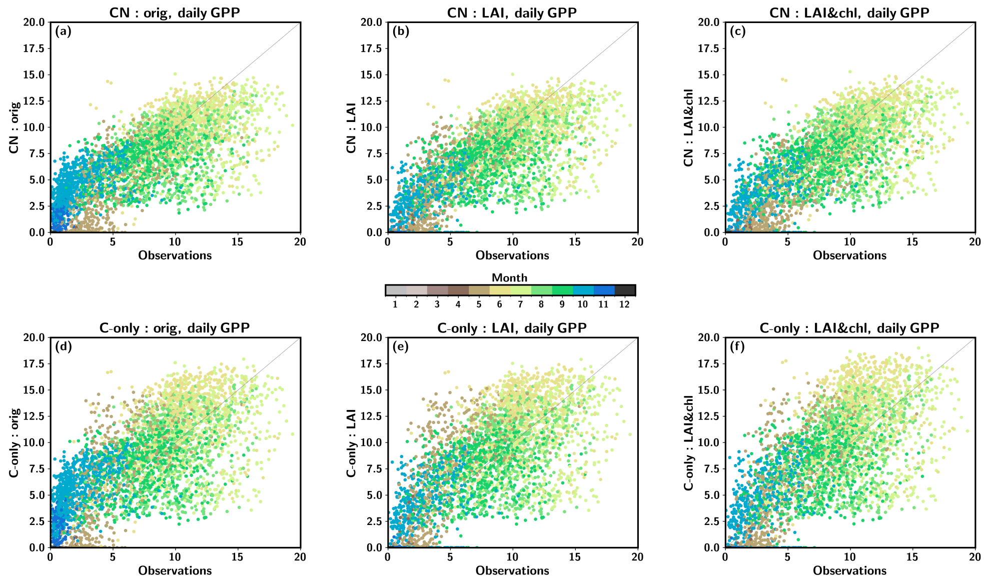


**Figure S3.** Scatter plot of observed daily (in units $\mu mol\,m^{-2}\,s^{-1}$) GPP vs. simulated daily GPP from the C-only:orig (d), C-only:LAI (e), C-only:LAI&chl (f), CN:orig (a), CN:LAI (b), CN:LAI&chl (c). The values for different months are denoted by different colors.

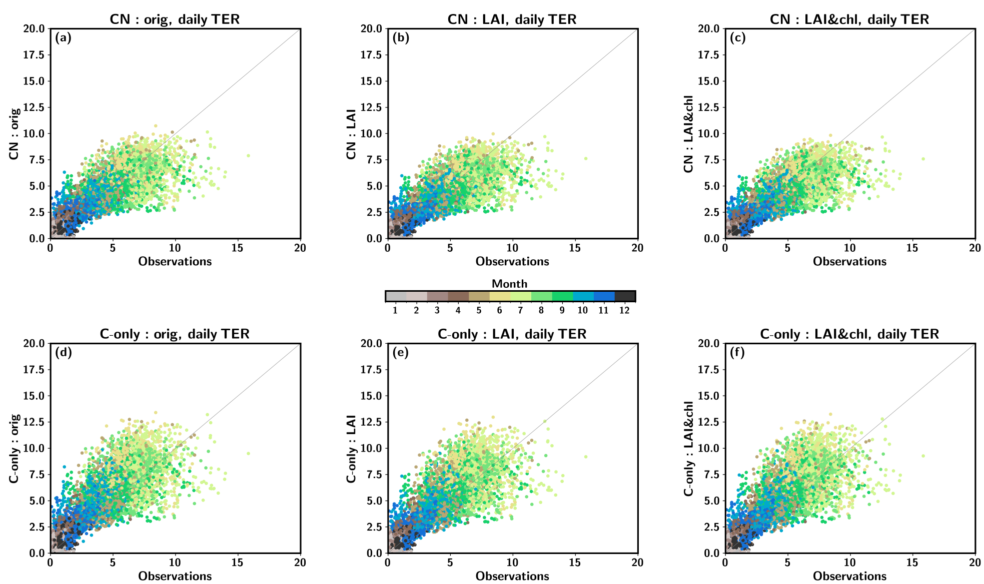


**Figure S4.** Scatter plot of observed daily (in units $\mu mol\,m^{-2}\,s^{-1}$) TER vs. simulated daily TER from the C-only:orig (d), C-only:LAI (e), C-only:LAI&chl (f), CN:orig (a), CN:LAI (b), CN:LAI&chl (c). The values for different months are denoted by different colors.

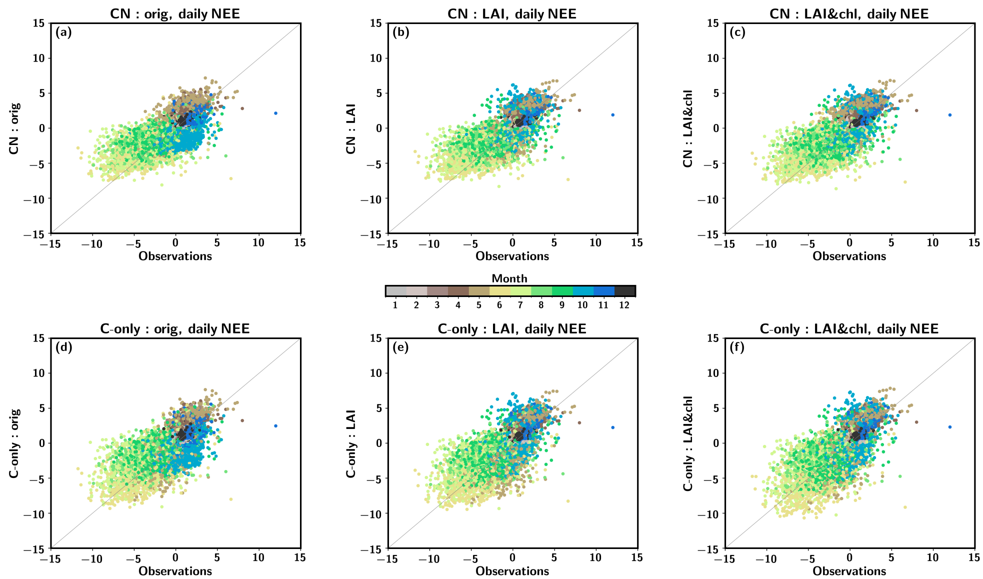


**Figure S5.** Scatter plot of observed daily (in units $\mu\mathrm{mol\,m^{-2}\,s^{-1}}$) NEE vs. simulated daily NEE from the C-only:orig (d), C-only:LAI (e), C-only:LAI&chl (f), CN:orig (a), CN:LAI (b), CN:LAI&chl (c). The values for different months are denoted by different colors.

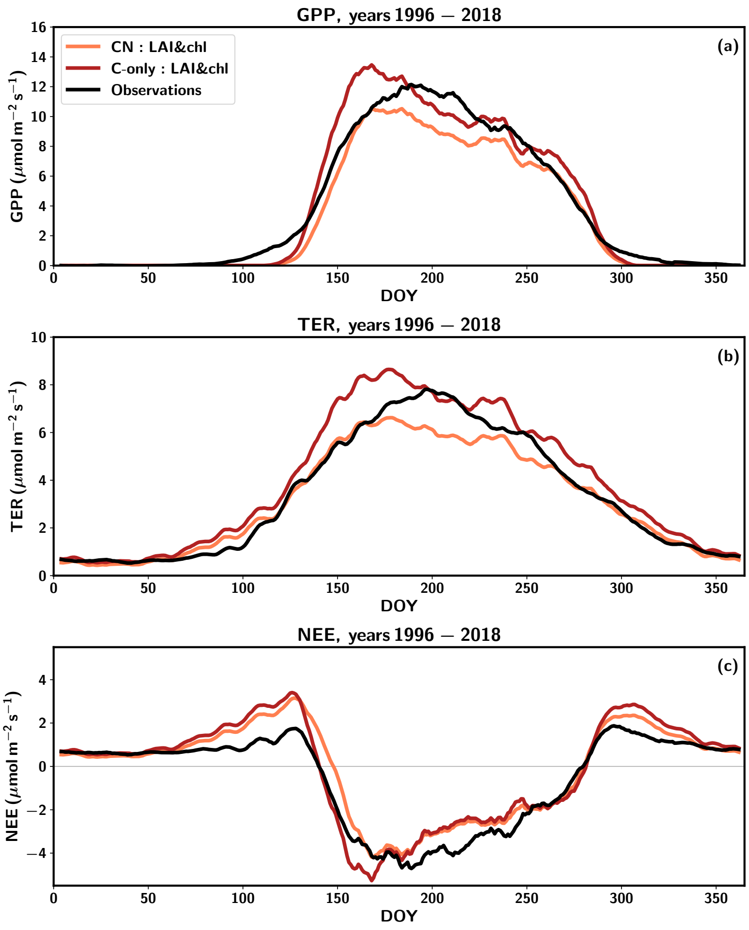


**Figure S6.** Averaged annual cycles of gross primary production, GPP (a), total ecosystem respiration, TER (b) and net ecosystem exchange, NEE (c) over 1996-2018. Observations are in black, the QUINCY results with C-only:LAI&chl in red and CN:LAI&chl simulations in orange. Both observations and model results have been smoothed with a seven-day averaging window.

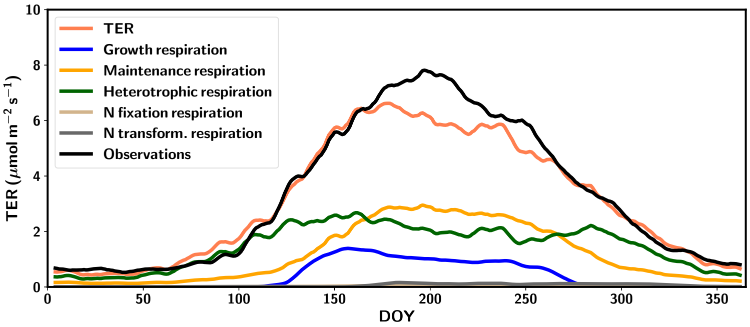


**Figure S7.** Seasonal cycle of the observed and simulated total ecosystem respiration (TER) from the CN:LAI&chl simulations, averaged over 1996-2018 and smoothed with a seven-day averaging window. The observation of TER in black, the simulated TER in magenta, the growth respiration in blue, the maintenance respiration in orange and heteotrophic respiration in dark green. The N fixation respiration is in beige and N transformation respiration is in grey.

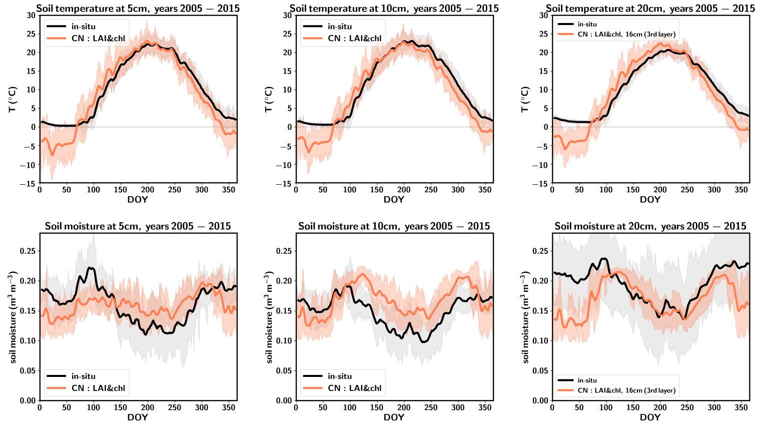


**Figure S8.** Seasonal cycles of soil temperature at depths of 5 cm (a), 10 cm (b) and 20 cm (c) and of soil moisture at depths of 5 cm (d), 10 cm (e) and 20 cm (f). The observations are in black and CN:LAI&chl simulations in orange. The standard deviations are shown as shaded regions. The results have been smoothed with a seven-day averaging window.

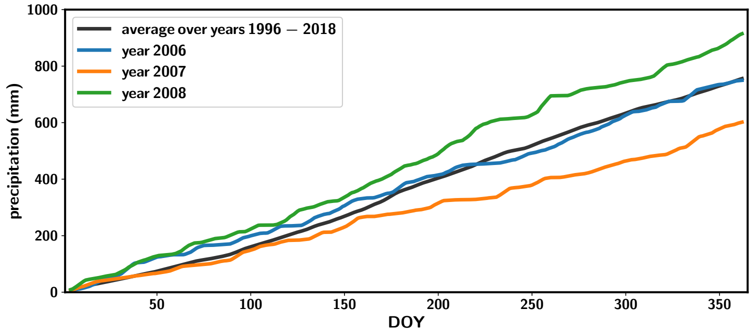


**Figure S9.** The cumulative rain fall, averaged for the years 1996-2018 (black line), year 2006 (blue line), year 2007 (orange line) and year 2008 (green line).

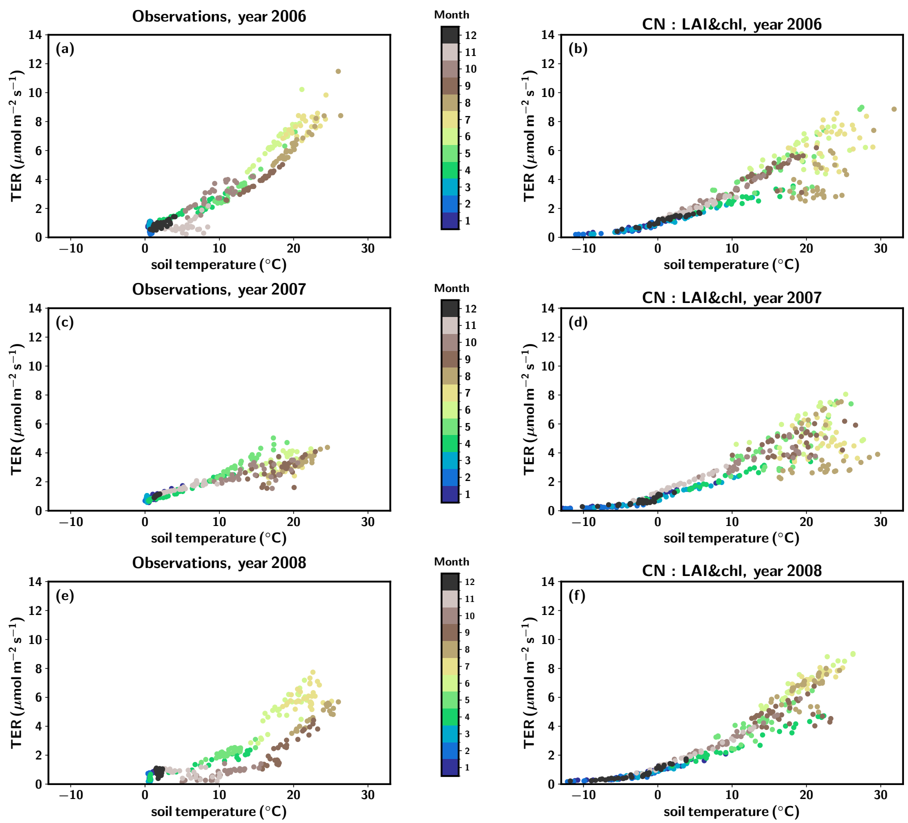


**Figure S10.** Total ecosystem respiration (TER) vs. soil temperature with color coding for different months. In (a, c, e) measurements for year 2006, 2007 and 2008, respectively. In (b, d, f) QUINCY results for 2006, 2007 and 2008, respectively.

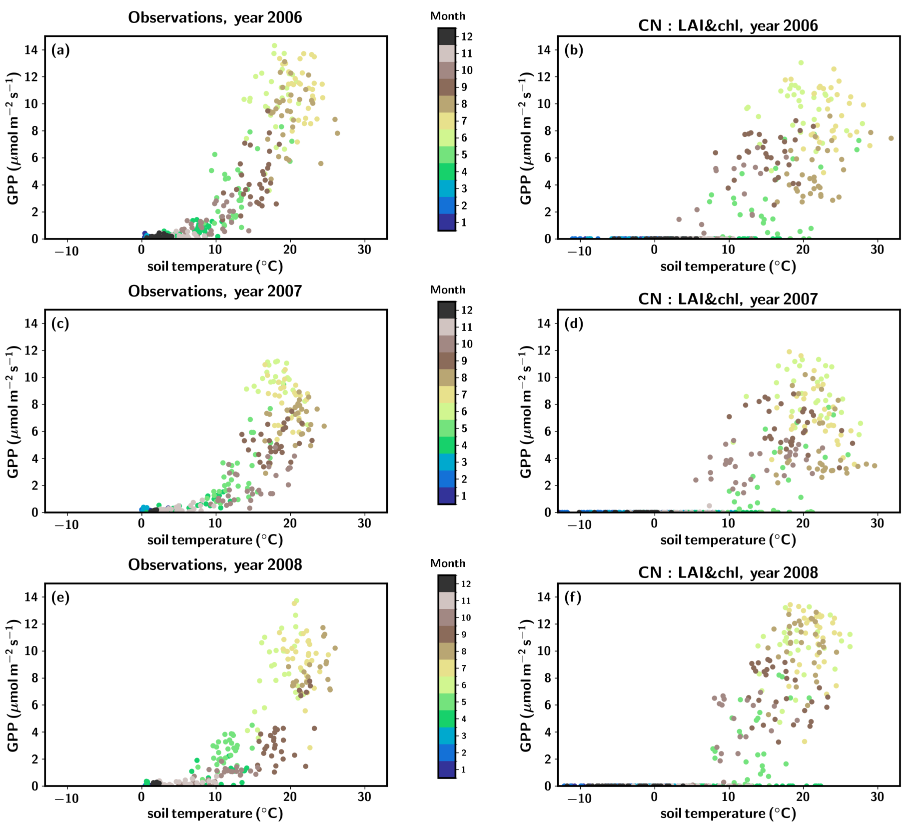


**Figure S11.** Gross primary production (GPP) vs. soil temperature with color coding for different months. In (a, c, e) measurements for year 2006, 2007 and 2008, respectively. In (b, d, f) QUINCY results for 2006, 2007 and 2008, respectively.

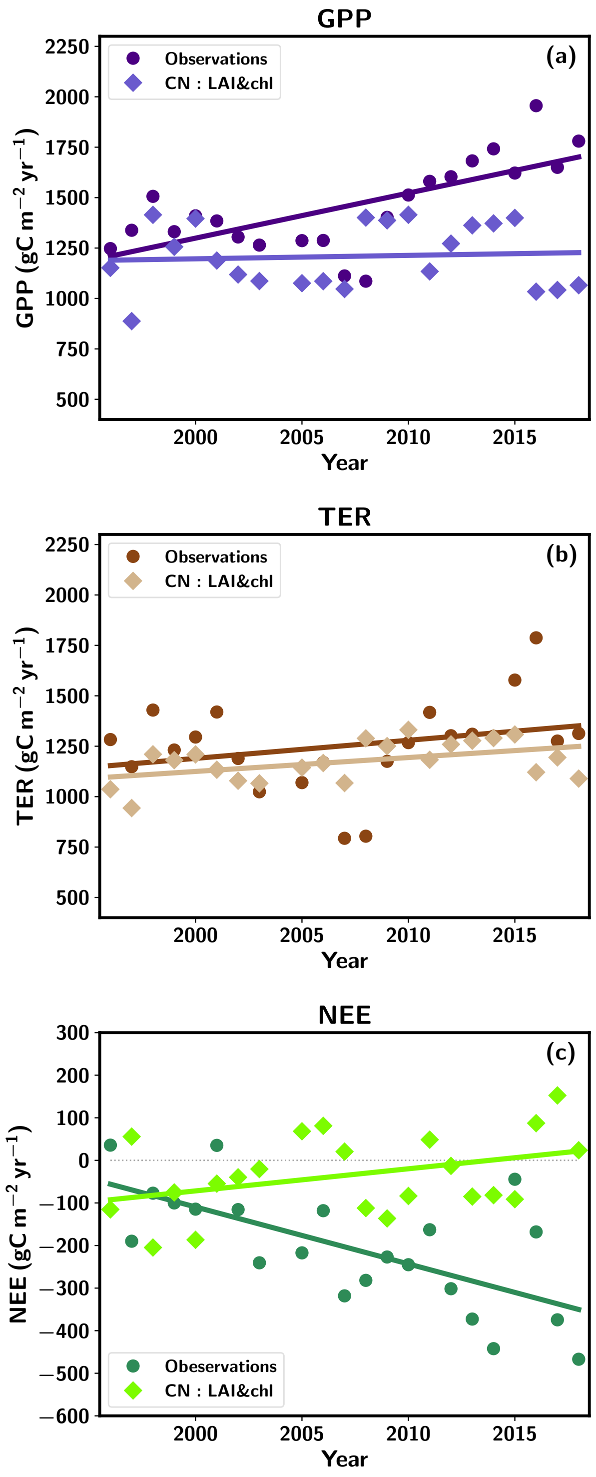


**Figure S12.** The annual values of GPP (a) (observations in violet circles, simulations in blue stars), TER (b) (observations in brown circles, simulations in light brown stars) and NEE (b) (observations in green circles, simulations in light green stars), with the fitted lines (the regression coefficients are given in Table S2.)

**Table S1.** Annual averaged carbon fluxes for different model parameterizations, together with their standard deviations, root mean square error (RMSE) and $r^2$ values. RMSE and $r^2$ have been calculated from the daily averages for the time period 1996-2018.

| GPP | Annual value ($\mathrm{gC\,m^{-2}yr^{-1}}$) | RMSE ($\mathrm{\mu mol\,m^{-2}\,s^{-1}}$) | $r^2$ (-) |
|---|---|---|---|
| Observation | 1459 ± 224 | - | - |
| C-only:orig | 1574 ± 189 | 2.58 | 0.71 |
| C-only:LAI | 1484 ± 184 | 2.50 | 0.72 |
| C-only:LAI&chl | 1511 ± 192 | 2.56 | 0.71 |
| C-only,fix:orig | 1243 ± 148 | 2.26 | 0.78 |
| C-only,fix:LAI | 1166 ± 144 | 2.22 | 0.78 |
| C-only,fix:LAI&chl | 1226 ± 158 | 2.19 | 0.79 |
| CN:orig | 1297 ± 171 | 2.23 | 0.78 |
| CN:LAI | 1225 ± 160 | 2.18 | 0.79 |
| CN:LAI&chl | 1209 ± 163 | 2.16 | 0.80 |
| **TER** | **Annual value ($\mathrm{gC\,m^{-2}yr^{-1}}$)** | **RMSE ($\mathrm{\mu mol\,m^{-2}\,s^{-1}}$)** | **$r^2$ (-)** |
| Observation | 1254 ± 220 | - | - |
| C-only:orig | 1534 ± 132 | 1.77 | 0.59 |
| C-only:LAI | 1450 ± 130 | 1.64 | 0.65 |
| C-only:LAI&chl | 1474 ± 133 | 1.68 | 0.63 |
| C-only,fix:orig | 1199 ± 96.6 | 1.41 | 0.74 |
| C-only,fix:LAI | 1129 ± 94.9 | 1.44 | 0.73 |
| C-only,fix:LAI&chl | 1187 ± 101 | 1.43 | 0.74 |
| CN:orig | 1255 ± 107 | 1.40 | 0.75 |
| CN:LAI | 1190 ± 101 | 1.39 | 0.75 |
| CN:LAI&chl | 1174 ± 100 | 1.38 | 0.75 |
| **NEE** | **Annual value ($\mathrm{gC\,m^{-2}yr^{-1}}$)** | **RMSE ($\mathrm{\mu mol\,m^{-2}\,s^{-1}}$)** | **$r^2$ (-)** |
| Observation | -205 ± 140 | - | - |
| C-only:orig | -40 ± 106 | 2.08 | 0.37 |
| C-only:LAI | -35 ± 100 | 2.01 | 0.42 |
| C-only:LAI&chl | -37 ± 106 | 2.06 | 0.39 |
| C-only,fix:orig | -44 ± 91 | 1.88 | 0.49 |
| C-only,fix:LAI | -37 ± 87 | 1.73 | 0.57 |
| C-only,fix:LAI&chl | -39 ± 95 | 1.81 | 0.53 |
| CN:orig | -42 ± 97 | 1.88 | 0.49 |
| CN:LAI | -36 ± 91 | 1.76 | 0.55 |
| CN:LAI&chl | -35 ± 94 | 1.78 | 0.54 |

**Table S2.** The regression coefficients with their uncertainty range and Pearson R for the observed and simulated carbon fluxes (1996-2018). JFM stands for January, February and March, AM for April and May, JJA for June, July and August, SO for September and October, ND for November and December. The values for the significant trends (where p < 0.05) are written in bold and marked with an asterisk. An dash denotes a value that was possible to determine.

| Flux observations | GPP | | TER | | NEE | |
|---|---|---|---|---|---|---|
| season | regr. coef | Pearson R | regr. coef | Pearson R | regr. coef | Pearson R |
| JFM ($gC\,m^{-2}\,month^{-1}yr^{-1}$) | -0.13 [-0.27 – 0.01] | -0.39 | 0.19 [-0.22 – 0.59] | 0.20 | 0.32 [-0.07 – 0.70] | 0.34 |
| AM ($gC\,m^{-2}\,month^{-1}yr^{-1}$) | 0.26 [-1.11 – 1.64] | 0.08 | 0.89 [-0.41 – 2.19] | 0.29 | 0.63 [-0.55 – 1.80] | 0.23 |
| JJA ($gC\,m^{-2}\,month^{-1}yr^{-1}$) | **5.76*** **[3.84 – 7.68]** | 0.80 | 1.16 [-1.40 – 3.71] | 0.20 | **-4.61*** **[-6.04 – -3.17]** | -0.82 |
| SO ($gC\,m^{-2}\,month^{-1}yr^{-1}$) | **2.59*** **[0.65 – 4.54]** | 0.51 | 1.19 [-0.84 – 3.22] | 0.25 | **-1.41*** **[-2.38 – -0.43]** | -0.54 |
| ND ($gC\,m^{-2}\,month^{-1}yr^{-1}$) | -0.13 [-0.39 – 0.14] | -0.21 | 0.40 [-0.22 – 1.01] | 0.28 | 0.53 [-0.01 – 1.06] | 0.40 |
| yearly (gC m-2 yr-1 yr-1) | **22.35*** **[11.88 – 32.83]** | 0.69 | 8.98 [-4.71 – 22.66] | 0.28 | **-13.38*** **[-20.15 – -6.61]** | -0.66 |

| QUINCY CN:LAI&chl | GPP | | TER | | NEE | |
|---|---|---|---|---|---|---|
| season | regr. coef | Pearson R | regr. coef | Pearson R | regr. coef | Pearson R |
| JFM ($gC\,m^{-2}\,month^{-1}yr^{-1}$) | 0.00 [0.00 – 0.00] | - | 0.20 [-0.16 – 0.56] | 0.24 | 0.20 [-0.16 – 0.56] | 0.24 |
| AM ($gC\,m^{-2}\,month^{-1}yr^{-1}$) | 0.68 [-1.17 – 2.53] | 0.16 | **1.02*** **[0.07 – 1.96]** | 0.43 | 0.34 [-0.82 – 1.49] | 0.13 |
| JJA ($gC\,m^{-2}\,month^{-1}yr^{-1}$) | -0.24 [-2.73 – 2.26] | -0.04 | 0.56 [-0.70 – 1.81] | 0.19 | 0.79 [-0.60 – 2.18] | 0.25 |
| SO ($gC\,m^{-2}\,month^{-1}yr^{-1}$) | 0.53 [-0.85 – 1.90] | 0.17 | **0.92*** **[0.22 – 1.63]** | 0.51 | 0.40 [-0.92 – 1.71] | 0.13 |
| ND ($gC\,m^{-2}\,month^{-1}yr^{-1}$) | 0.00 [0.00 – 0.00] | 0 | 0.38 [-0.22 – 0.97] | 0.27 | 0.38 [-0.22 – 0.97] | 0.27 |
| yearly (gC m-2 yr-1 yr-1) | 1.70 [-8.79 – 12.20] | 0.07 | **6.90*** **[1.16 – 12.64]** | 0.47 | 5.20 [-0.39 – 10.78] | 0.38 |